Journal of Hazardous Materials 435 (2022) 128884

Contents lists available at ScienceDirect

Journal of Hazardous Materials

journal homepage: www.elsevier.com/locate/jhazmat

Research Paper

Microplastics exposure affects neural development of human pluripotent stem cell-derived cortical spheroids

Timothy Hua [a,1], Sonia Kiran [a,1], Yan Li [b,*], Qing-Xiang Amy Sang [a,**]

[a] Department of Chemistry and Biochemistry, Florida State University, Tallahassee, FL, United States
[b] Department of Chemical and Biomedical Engineering, FAMU-FSU College of Engineering, Florida State University, Tallahassee, FL, United States

HIGHLIGHTS

- Microplastics (MPs) have negative impact on human forebrain organoid development.
- Short-term exposure promotes cell proliferation and neural progenitor gene expression.
- Long-term exposure reduces cell viability.
- Long-term exposure downregulates mature neuronal marker and cortical layer VI marker.

GRAPHICAL ABSTRACT

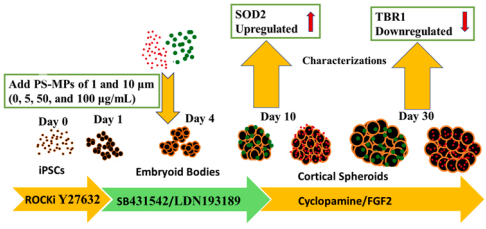

ARTICLE INFO

Editor: Nan Sang

Keywords:
Microplastics
Human pluripotent stem cells
Neural differentiation
Cortical organoids
Oxidative stress

ABSTRACT

Plastics have been part of our ecosystem for about a century and their degradation by different environmental factors produce secondary microplastics (MPs). To date, the impact of MPs on human health has not been well investigated. To understand the possible effects of polystyrene-MPs (PS-MPs) on the human brain, a 3D model of human forebrain cortical spheroids has been derived, which mimics early development of human cerebral cortex. The spheroids were exposed to 100, 50, and 5 μg/mL of 1 μm and 10 μm PS-MPs during day 4–10 and day 4–30. The short-term MP exposure showed the promoted proliferation and high gene expression of *Nestin, PAX6, ATF4, HOXB4* and *SOD2*. For long-term exposure, reduced cell viability was observed. Moreover, changes in size and concentration of PS-MPs altered the gene expression of DNA damage and neural tissue patterning. In particular, *β-tubulin III, Nestin*, and *TBR1/TBR2* gene expression decreased in PS-MP treated conditions compare to the untreated control. The results of this study suggest that the size- and concentration-dependent exposure to PS-MPs can adversely affect embryonic brain-like tissue development in forebrain cerebral spheroids. This study has significance in assessing environmental factors in neurotoxicity and degeneration in human.

1. Introduction

The production of plastic increases each year by 300 million ton (Mendes et al., 2021). Different environmental factors such as chemical, mechanical and biological properties degrade these plastics into microplastics (Corcoran, 2020; Yuan et al., 2020). These microplastic particles (MPs) can easily be transported through air and water to become part of the ecosystem, affecting land as well as marine

* Correspondence to: 2525 Pottsdamer St., Tallahassee, FL 32310, United States.
** Correspondence to: 102 Varsity Way, Tallahassee, FL 32306, United States.
E-mail addresses: tph16c@my.fsu.edu (T. Hua), sk19bc@my.fsu.edu (S. Kiran), yli4@fsu.edu (Y. Li), qxsang@chem.fsu.edu (Q.-X.A. Sang).
[1] Co-first authors

https://doi.org/10.1016/j.jhazmat.2022.128884
Received 9 December 2021; Received in revised form 31 March 2022; Accepted 7 April 2022
Available online 11 April 2022

organisms (Rochman, 2018). These MPs enter the body of the living organisms through inhalation and ingestion and can circulate to deposit in various organs, such as brain (e.g., the degraded nanoscale plastics have the possibility to cross blood brain barrier), lungs, stomach, liver, and kidney (Abrahams, 2002; Dehghani et al., 2017; Prüst et al., 2020; Yin et al., 2018). Some polystyrene MPs are detected in fetal liver, lung, brain and other organs, circulating from maternal lungs via the placenta of pregnant rats (Fournier et al., 2020). To date, the effects of environmental MPs (1–5 μg/mL) on human health have not been well understood yet, but some studies have shown the presence of MPs in various organs like lungs and placenta (Meyer et al., 2018; Ragusa et al., 2021). Microplastic contamination has adverse effects on the environment and can cause serious health problems in living organisms (Franzellitti et al., 2019; Luo et al., 2019; Mammo et al., 2020; Prüst et al., 2020), therefore, in-depth studies to investigate these effects and mechanism of toxicity in human model systems are urgently needed.

Polystyrene MPs (PS-MPs) have been frequently observed in marine and land organisms (Ding et al., 2018; Lei et al., 2018; Long et al., 2017; Lu et al., 2018; Luo et al., 2019; Qu and Wang, 2020). It was observed that epithelial cells of lungs exposed to PS-MPs showed disruption of junction proteins and may lead to dysfunction of the pulmonary barrier (Dong et al., 2020). At the organism level, people who work at the manufacturing facilities that are close to the fumes of styrene suffered from acute respiratory symptoms and bronchiolitis (Meyer et al., 2018). The polystyrene plastic particles may enter the brain through the olfactory system (nose) or circulatory system (lungs and guts) (Prüst et al., 2020). Specifically, the polystyrene particles below 100 nm can transport through axons of olfactory nerve (Mistry et al., 2009). They also can enter trigeminal and olfactory nerve, and pass through the olfactory tract into the brain (Ahmad et al., 2017). One of the proposed mechanisms of PS-MPs cytotoxicity is the increased oxidative stress, cellular stress, and activating p38 mitogen-activated protein kinase pathway (Xie et al., 2020).

Reactive oxidative species (ROS) production is the most common effect of toxicity when the cells are exposed to environmental pollutants such as nanoparticles, microplastics, and UV radiations by disturbing the balance of redox potential of the cells and producing more oxidative chemicals (Fetoni et al., 2021; Liang et al., 2017; Sheng et al., 2015; Wu et al., 2018). ROS mainly include peroxides, superoxides, hydroxyl radicals, and some reactive nitrogen species (Singh et al., 2019). These chemicals can do heavy damage not only to the brain but also to other organs, altering the cell nucleic acid and other macromolecules, proteins, lipids as well as causing mitochondrial malfunctioning (Chandrasekaran et al., 1994; Freeman and Keller, 2012; Maurer et al., 2000; Nagy et al., 1999; Singh et al., 2019).

The human central nervous system is highly vulnerable to environmental toxins during embryonic development (Rice and Barone, 2000). Exposing neurons to MPs could result in the increased ROS production, leading to cellular damage and the increased neuroinflammation in the brain (Prüst et al., 2020). Also, MP exposure could inhibit acetylcholinesterase and change the neurotransmitter levels, which would contribute to the behavioral changes (Prüst et al., 2020). The neurotoxicity of microplastics has been one of the crucial concerns recently because of the possible neurotoxicity by PS and other MPs observed in studies involving marine and land animals (Barboza et al., 2020, 2018; Chen et al., 2017; Lei et al., 2018; Qu and Wang, 2020; Rafiee et al., 2018).

Human induced pluripotent stem cells (hiPSCs)-derived brain organoids (or spheroids) have emerged recently as a promising platform for neurological disease modeling and drug screening studies (Chiaradia and Lancaster, 2020; Del Dosso et al., 2020; Garreta et al., 2021; Kyrousi and Cappello, 2020; Velasco et al., 2019). The novel brain organoid models at least partially recapitulate the embryonic brain tissue development and can carry genetic background of the parent donors (Cederquist et al., 2019; Kyrousi and Cappello, 2020). To better understand the possible neurotoxicity of polystyrene microplastics in humans, this study has investigated an in vitro 3D model of human forebrain cerebral spheroids/organoids derived from hiPSCs, which have been characterized in our previous studies (Song et al., 2019a, 2019b; Yan et al., 2018a, 2018b). Our previous studies have also used this hiPSC-derived 3D cortical spheroid model in evaluating the effects of nanoscale iron oxides (Henderson et al., 2022), microglia functionalization, and extracellular matrix alterations for neural degeneration study (Bejoy et al., 2018a; Marzano et al., 2021; Song et al., 2019b). These cerebral spheroids which were developed after 4 weeks of differentiation, mainly consist of neuronal progenitor cells and neurons. In this study, from day 4 to day 10 (short-term) or day 4 to day 30 (long-term), the cortical spheroids were exposed to 1 and 10 μm PS-MPs with various concentrations of 5, 50, and 100 μg/mL. This range of concentration was chosen based on the environmental relevance, our previous study of MPs on lung cells with a range of MP concentrations (Goodman et al., 2021), the need to complete the investigations with limited experimental span (e.g., one month), as well as the range (up to 250 μg/mL) reported in current literature (Prüst et al., 2020; Stock et al., 2019). To investigate the effects of PS-MP exposure on the development of the forebrain spheroid model, qualitative and quantitative analysis at protein and molecular levels of the biomarkers for cell proliferation, ROS enzyme, cell viability, cell death, neural progenitors, cortical layer, and neuronal cells were performed. This study has significance in neurotoxicity study and advances our understanding of the health impact or threat of environmental microplastics in-vitro human models (Miloradovic et al., 2021).

2. Materials and methods

2.1. Undifferentiated human iPSC culture

The iPSK3 cell line was obtained by transfecting human foreskin fibroblasts with plasmid DNA encoding reprogramming factors octamer-binding transcription factor 4 (OCT4), NANOG, SRY-box transcription factor 2 (SOX2), and LIN28 (kindly provided by Dr. Stephen Duncan, Medical College of Wisconsin) (Si-Tayeb et al., 2010; Si-Tayeb et al., 2010). The cells were cultured in mTeSR Plus serum free medium (StemCell Technologies, Inc., Vancouver, Canada) on growth factor-reduced Matrigel-coated surface (Life Technologies). They were passage every seven days using Accumax and seeded at 1×10^6 cells per well of 6-well plate. Rho-associated protein kinase (ROCK) inhibitor Y27632 (10 μM, Sigma) was used for the first 24 h to promote higher survival (Bejoy et al., 2018b; Song et al., 2016; Yan et al., 2015).

2.2. Differentiation of hiPSCs into forebrain cortical spheroids

Undifferentiated human iPSK3 cells were seeded into Ultra-Low Attachment (ULA) 24-well plates (Corning Inc., Corning, NY) at 3×10^5 cells/well in differentiation medium composed of Dulbecco's Modified Eagle Medium: Nutrient Mixture F-12 (DMEM/F12) plus 2% B27 serum-free supplement (Life Technologies, Carlsbad, CA). iPSK3 cells were seeded in the presence of ROCK inhibitor Y27632 (10 μM). After 24 h, Y27632 was removed and the formed embryoid bodies (EB) were treated with dual SMAD signaling inhibitors of 10 μM SB431542 (Sigma-Aldrich, St. Louis, MO) and 100 nM LDN193189 (LDN, Sigma) over 7 days. Then on day 8, the spheroids were treated with fibroblast growth factor (FGF)− 2 (10 ng/mL, Life Technologies) and cyclopamine (an Sonic hedgehog (Shh) inhibitor, 1 μM, Sigma) for cortical differentiation for a total of 30 days (Song et al., 2019a; Yan et al., 2016, 2018b). From day 4 of the culture, the media was supplemented with 2% B27 without antioxidants (Life Technologies). The day 10 or day 30 spheroids were replated on Matrigel for further analysis.

2.3. MP characterization by Fourier Transform Infrared (FTIR) spectroscopy

Different sizes (1 or 10 μm, i.e., MP1 and MP10) of sterilized microplastics (Degradex product) were obtained from Phosphorex, Inc. (Hopkinton, MA). The MPs were prepared in 0.2 um filtered water. FTIR analysis of MPs was performed to verify the functional group composition of 1 or 10 μm PS-MPs using JASCO 6800 FT-IR Spectrometer with Transmittance ATR. Dichloromethane or toluene was added to the microplastics that were suspended in water before mixing vigorously. The organic layer that contained partially dissolved polystyrene was separated and dried with $MgSO_4$ before analyzing with FTIR. The mid-IR range with wavenumber between 250 and 6000 cm^{-1} was chosen and about 55–65 scans were taken to minimize the noise. The background spectrum was measured before loading the sample, then 3 μL microplastic suspension of 10 mg/mL was placed on the diamond crystal of ATR. The spectra shown is processed after baseline correction, noise elimination, and smoothing.

2.4. Dynamic light scattering (DLS) analysis of MPs

To find actual size and polydispersity index of and 1 and 10-micron microplastics in the cell culture media (DMEM/F12), DLS analysis was performed using the software with stokes-Einstein equation to measure the hydrodynamic radius (Lim et al., 2013). Briefly, the sample was loaded in the DLS tube, which was rinsed with toluene to minimize the noise. The tube with the sample was placed in the ALV/CGS-3 compact goniometer instrument that was connected to ALV-7004 correlator software to run the sample and analyze the results. Before DLS was measured, all the parameters were set for DMEM media such as the refractive index (1.4150), Angle (90), and viscosity (0.89 cp). After running the sample, the correlation function and the distribution function were regularized. The graph of distribution function obtained displayed actual hydrodynamic radius, while the polydispersity index (PDI) was obtained after cumulant fit.

2.5. Cortical spheroid exposure to MPs and MP accumulation analysis

On day 4 of cortical spheroid differentiation, the culture was fed with media containing 5, 50, and 100 μg/mL of MP1 or MP10. The control condition was the parallel culture that did not expose to any MPs. The MP-containing media were changed every 2–3 days up to day 10 or day 30 for further characterizations. For measuring the MP accumulation in the cells, the spheroid culture was treated with fluorophorex, the fluorescent microspheres of size 1 and 10 μm from phosphorex Inc. After 10 days of microplastic exposure, the culture of spheroids was treated with Accumax to obtain a single cell suspension. The dissociated cells were fixed for flow cytometry. The flow cytometry was performed using BD FACSCanto™ II flow cytometer (Becton Dickinson) instrument and analyzed against the control (i.e., no MP exposure) using FlowJo software.

The effects of PS-MP leachate were also investigated. Briefly, the MP1 and MP10 were added to the DMEM/F12 media at 5, 50, and 100 μg/mL and incubated for 5 days at 37 °C. On day 5, the media were separated from microplastics through high-speed centrifugation. These media (i.e., leachate) were added to the day 10 developing cortical spheroids and the cultures were maintained for another 4 days. Then, the flow cytometry was performed on the dissociated cortical spheroids to measure the expression of SOD2 and Ki67. The culture not exposed to the leachate was used as the untreated control.

2.6. Aggregate size distribution

The images of cortical spheroids (both the MP-treated and the untreated control) were captured at day 28 by a phase contrast microscopy. The captured images were converted to binary images using ImageJ software (http://rsb.info.nih.gov/ij) and analyzed with the "particle analysis tool". Through particle analysis in ImageJ software, the Feret's diameter of each aggregate in the images was calculated to provide the size distribution of the aggregates.

2.7. Live/dead staining for flow cytometry

The cells were evaluated for viability using the Live/Dead™ staining kit (Molecular Probes) according to the manufacturer's protocol. After treating with microplastics, the spheroids were trypsinized, washed with phosphate-buffered saline (PBS) and then incubated in DMEM-F12 containing 3–10 μM calcein-AM (green) and 8 μM ethidium homodimer I (red) for 20 min at room temperature and protected from light. The cells were acquired by flow cytometry for quantification.

2.8. Immunocytochemistry

For biomarker detection, the cells were fixed using 5% paraformaldehyde (PFA) and permeabilized using 0.2% Triton-X 100. The samples were blocked with 5% FBS in PBS and stained with the primary antibodies (Supplementary Table S1), followed by the corresponding anti-species Alexa Fluoro antibodies, i.e., Alexa Fluor 488 goat anti-mouse IgG1 or Alexa Fluor 594 goat anti-Rabbit IgG (Life technologies). Both primary and secondary antibody dilutions were made based on the manufacturer's recommendations and prepared in staining buffer (2% FBS in PBS). Then the nuclei were counterstained with Hoechst 33342 (blue), and pictures were taken for blue, green, and red colors to detect the markers and their cellular locations.

2.9. Flow cytometry for cellular phenotyping

To quantify various markers, the cells were dissociated using Accumax and analyzed by flow cytometry. Briefly, 1×10^6 cells per sample were fixed with 4% PFA and washed with PBS. The cells were permeabilized with 100% cold methanol, blocked with blocking buffer, and then incubated with various primary antibodies (Supplementary Table S1) followed by the corresponding secondary antibody Alexa Fluor 488 goat anti-Mouse IgG_1 or Alexa Fluor 594 Goat Anti-rabbit or Donkey Anti-Goat IgG. The cells were acquired with BD FACSCanto™ II flow cytometer (Becton Dickinson) and analyzed against isotype controls using FlowJo software.

2.10. Reverse transcription-polymerase chain reaction (RT-PCR) analysis

Total RNA was isolated from the neural cell samples exposed to MPs using the RNeasy Mini Kit (Qiagen, Valencia, CA) according to the manufacture's protocol, followed by treatment with the DNA-Free RNA Kit (Zymo, Irvine, CA). Reverse Transcription was carried out using 2 μg of total RNA, anchored oligo-dT primers, and Superscript III (Invitrogen, Carlsbad, CA, according to the manufacturer's protocol). Primers were specific to the targeted gene (Supplementary Table S2 and S3). The primers were designed using the software Primer-BLAST (NIH Database). The gene *β-actin* was used as an endogenous control for the normalization of expression levels. RT-PCR reactions were performed on an ABI7500 instrument (Applied Biosystems, Foster City, CA), using SYBRI Green PCR Master Mix (Applied Biosystems). The amplification reactions were performed as follows: 2 min at 50 °C; 10 min at 95 °C; and 40 cycles of 95 °C for 15 s; 55 °C for 30 s; and 68 °C for 30 s. The Ct values of the target genes were firstly normalized to the Ct values of the endogenous control *β-actin*. The corrected Ct values were then compared for the treatment conditions to the untreated control. Fold changes in gene expression was calculated using the comparative Ct method: $2^{-(\Delta C_{t\ treatment} - \Delta C_{t\ control})}$ to obtain the relative expression levels.

2.11. Statistical analysis

Each experiment was carried out at least three times with more than six replicates. The representative experiments were presented, and the results were expressed as [mean ± standard deviation]. To assess the statistical significance, one-way or two-way ANOVA followed by Fisher's LSD post hoc tests were performed. A p-value < 0.05 was considered statistically significant.

3. Results

3.1. Effects of short-term microplastics exposure at cellular level

The morphology of microplastics of 1 μm (MP1) and 10 μm (MP10) is shown in Supplementary Fig. S1**.** FTIR analysis confirmed the polystyrene identity of the MPs (Supplementary Fig. S2). The major peak of the aromatic ring (–C-H) was detected between 2700 and 2900 cm^{-1}, while the aliphatic (–C-H) is around 3000 cm^{-1}. The aromatic C═C is detected around 1550 cm^{-1} (Vardhan and Shukla, 2018). DLS analysis was performed to show that MPs do not aggregate in the culture (Supplementary Fig. S3). However, the MP10 can degrade into smaller particles (less than 2 μm) after more than 15 days in culture media. Different samples of MP1 and MP10 at 5 μg/mL, 50 μg/mL, and 100 μg/mL were also acquired using flow cytometry. Both sizes of MPs show higher events at higher concentrations. **(**Supplementary Fig. S4**).**

In this study, the two MP sizes were chosen to illustrate different interaction mechanisms with the cells. MP10 is in the similar size range compared to the cells and should stay in the extracellular space among the cells in the spheroids (Fig. 1**A**). MP1 can be uptaken by the cells as shown in our previous study (Goodman et al., 2021). The MP accumulation in the cells after 10 days was quantified by flow cytometry using the fluorescent MPs (Supplementary Fig. S5). For MP1, the uptake by the cells increased with the exposure concentration. At 5 μg/mL, only 3–4% cells contained MPs, while the percentage increased to 30% at 50 μg/mL and 77–81% at 100 μg/mL. For MP10, less than 5% of cells were positive at 5, 50, or 100 μg/mL. From the fluorescent images, MP1s could form an aggregate in the medium if the exposure time is long (Supplementary Fig. S6), but the aggregate was not observed in culture as seen in Supplementary Fig. S3 because the media were changed every 3–4 days after vortexing the microplastics. MP10 showed the distinct single particles. The cortical spheroids exposed to MP1 and MP10 did not show significant morphology alterations over the differentiation (Fig. 1**B** and Supplementary Fig. S7). Upon replating, some MPs can be seen among or inside the cells that migrated out of the spheroids **(**Fig. 1**C).**

The cortical spheroids were exposed to MP1 and MP10 at different concentrations (5, 50, and 100 μg/mL) during day 4–10 **(**Fig. 2A). For the untreated control, the day 6, 8 and 10 cells showed abundant proliferation marker Ki67 expression, minimal neuronal marker β-tubulin III expression, and abundant SOD2 (the enzyme involved in the ROS clean up) expression (Supplementary Fig. S8). Quantification of Ki67 and SOD2 using flow cytometry indicates 48–49% Ki67+ cells and 62–76% SOD+ expression for cells at day 6–10 (Supplementary Fig. S9). The replated cortical spheroids were evaluated by immunocytochemistry for neural progenitor markers Pax6 and Nestin expression (Fig. 2B). All the conditions showed normal phenotypic Pax6 and Nestin expression.

The Ki67 and SOD2 expression for cortical spheroids exposed to MP1 and MP2 at 5, 50, and 100 μg/mL was quantified by flow cytometry (Fig. 3 and Supplementary Fig. S10). The Ki67 showed the elevated expression of 78–86% for MP1 exposure and 65–79% expression for MP10 exposure, compared to the untreated control. The SOD2 expression was comparable (67–72%) to the untreated control except for MP1 at 50 μg/mL (35.3%). For MP10 exposure, similar results were observed with comparable SOD2 expression (60–81%) except for MP10 at 50 μg/mL (54.6%). Taken together, cortical spheroid exposure to MPs during day 4–10 showed normal neural differentiation, higher proliferation, and retained SOD2 expression.

3.2. Effects of short-term microplastics exposure at molecular level

To evaluate the microplastics effects at the molecular level, 10 different genes were measured by RT-PCR for cortical spheroids exposed to MP1 and MP10 at different concentrations during day 4–10 (Fig. 4 and Supplementary Table S2-S3). *ATF4* is a DNA binding protein that is expressed in neural progenitors. All the MP1 and MP10 conditions upregulated *ATF4* expression (1.2–1.6 fold) compared to the untreated control (Fig. 4**A**). Similarly, all the MP1 and MP10 (except for MP10 at 5 μg/mL) upregulated *Nestin* expression (1.2–1.6 fold) compared to the untreated control. For *PAX6*, all the MP1 and MP10 conditions upregulated the expression (~1.5 fold) compared to the untreated control (Fig. 4B). For *HOXB4* patterning, similar or higher (1.5–3.0 fold) expression was observed for the MP conditions compare to the control. *SOD2* gene expression was upregulated (1.2–2.0 fold) for all the MP conditions too (Fig. 4C). Another ROS-related gene *CAT* showed some variations, MP1 conditions had similar or higher (1.1–1.3 fold) expression, while MP10 conditions had similar or lower (~0.25 fold) expression. *CDKN1B* encodes cyclin-dependent kinase inhibitor 1B ($p27^{Kip1}$). It had similar expression for most MP conditions except for the 5 μg/mL exposure (1.6–2.0 fold) (Fig. 4D). Cell proliferation gene *MKI67* had similar or higher (1.2–1.7 fold) expression for MP conditions, and cell death-related gene *CAPS3* had similar expression in general (Fig. 4E). For sub-ventricular region marker *TBR2,* however, the expression level was similar for MP1 conditions or lower (0.1–0.4) for MP10 conditions. Taken together, MP exposure during day 4–10 of cortical spheroids promotes the expression of neural progenitor genes, elevated *SOD2* expression, and may affect *TBR2* expression.

3.3. Effects of long-term microplastics exposure at cellular level

The cortical spheroids were exposed to MP1 and MP10 at different concentrations (5, 50, and 100 μg/mL) during day 4–30 **(**Fig. 5A). At day 30, immunocytochemistry of neuronal marker β-tubulin III, proliferation marker Ki67, and SOD2 was performed (Fig. 5B and Supplementary Fig. S11-S12). Abundant β-tubulin III+ cells with axons were observed (much more than day 10 cells) and retained Ki67 as well as SOD2 expression were observed.

The quantification of Ki67, SOD2, and cortical layer VI marker TBR1 was performed by flow cytometry (Fig. 6). MP1 exposure showed the similar Ki67 expression (53.5–61.3%) compared to the untreated control (49.0%). For MP10 exposure, lower Ki67 expression was observed for 5 and 50 μg/mL conditions (17.1% and 33.1% respectively) but not 100 μg/mL condition (51.5%) (Fig. 6A). For SOD2, similar or higher expression (40.5%−74.0%) was observed for all MP conditions compared to the untreated control (41.5%). In particular, the 50 μg/mL MP1 and MP10 conditions showed the 65.8% and 74.0% of SOD2+ cells (Fig. 6B). For TBR1, the untreated control had high expression of 79.7%, while the MP1 exposure had 47.2–56.9% of TBR1+ cells and the MP10 exposure also had the lower percentage (17.0–36.6%) of TBR1+ cells (Fig. 6C).

The day 30 cortical spheroids exposed to MP1 and MP10 at different concentrations (5, 50, and 100 μg/mL) were analyzed using Live/Dead cell quantification with flow cytometry (Fig. 7). Q3 (or Q2 +Q3) represents the live cells. For MP1 conditions, the concentration of 5, 50, and 100 μg/mL reduced the percentage of live cells (51.5%, 29.7%, and 39.6% respectively) compared to the untreated control (61.6%). For MP10 conditions, a lower percentage of live cells (47.5% and 29.6% respectively) was observed for 5 and 50 μg/mL conditions, but the 100 μg/mL condition (64.2%) showed the comparable viability to the untreated control (61.6%). Taken together, MP1 exposure reduced the cell viability of day 30 cortical spheroids.

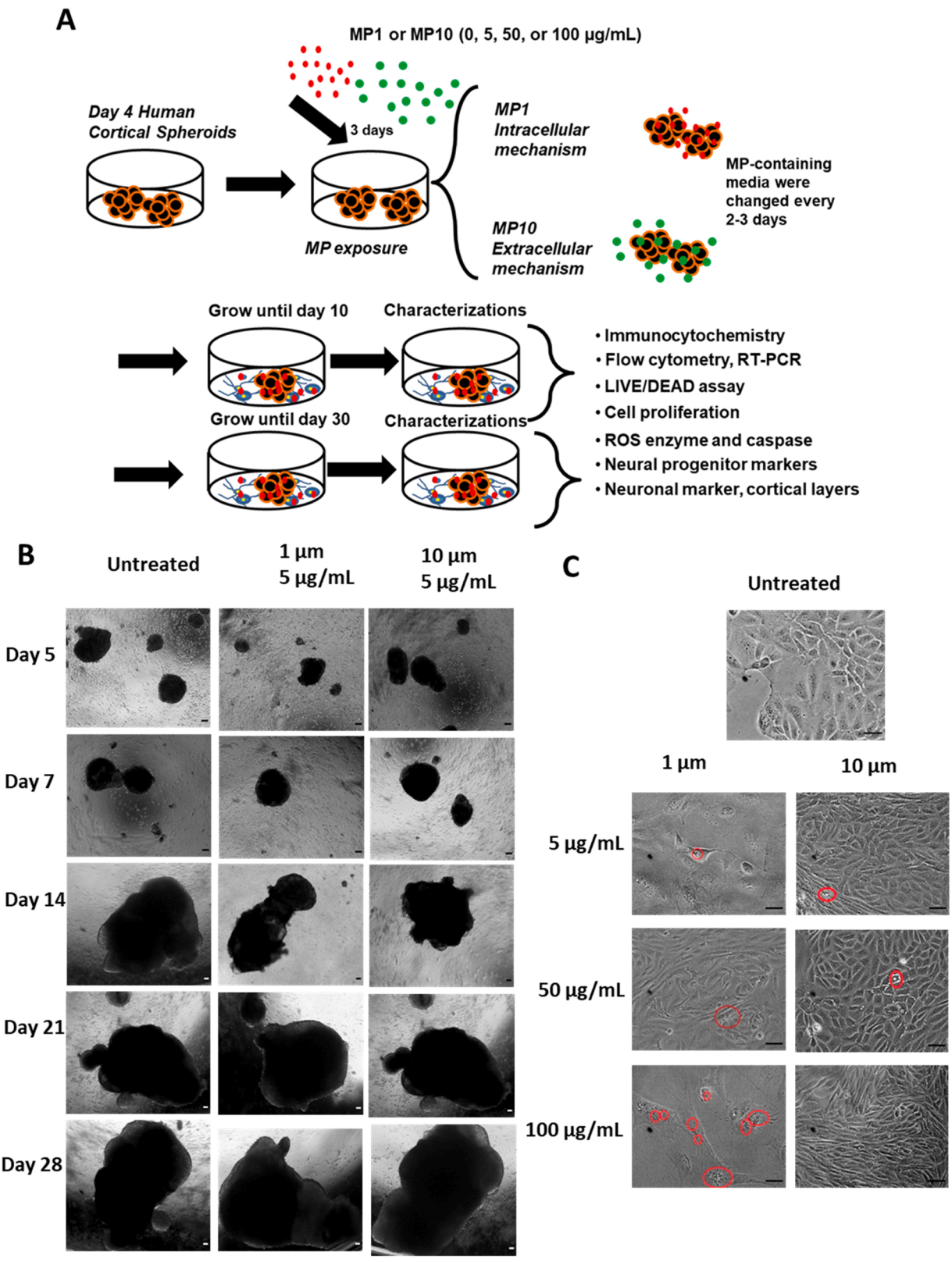

Fig. 1. Morphology of microplastics and their interactions with forebrain cortical spheroids. (A) Schematic illustration of the study design; MP1: microplastic particles of 1 µm (µm) in size; MP10: microplastic particles of 10 µm (µm) in size. (B) Phase contrast images of forebrain cortical spheroids exposed to microplastics and the phase contrast images were taken with 4X objective to give the overview of the spheroids. Scale bar: 20 µm. (C) Spheroids replated on Matrigel on day 30 for another 10 days and phase contrast images were taken with 20X objective. Red circles show the presence of MPs in the culture. Scale bar: 100 µm.

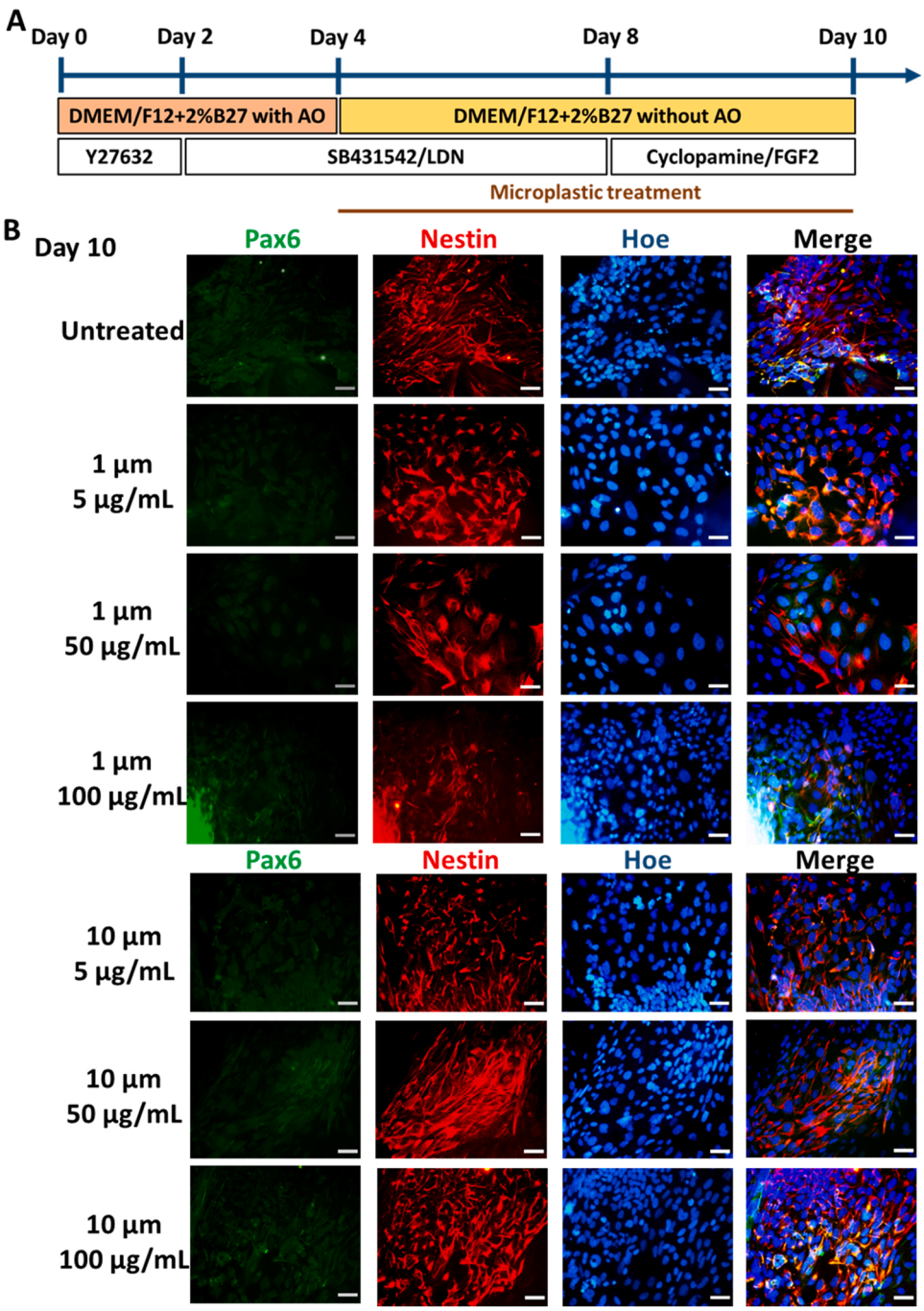

Fig. 2. Immunocytochemistry for the expression of Pax6 and Nestin in day 10 cortical spheroids exposed to MPs. (A) Schematic illustration of the spheroid exposure to 1 μm and 10 μm MPs at different concentrations (5, 50, and 100 μg/mL) during day 4–10. The spheroids were then replated on Matrigel-coated surface for immunocytochemistry. (B) The images shown the individual as well as the merged view of the expression of Pax6 and Nestin in the cells exposed to 1 μm and 10 μm MPs. Blue: Hoechst 33342. Scale bar: 100 μm.

3.4. *Effects of long-term microplastics exposure at molecular level*

To evaluate the microplastics effects at the molecular level for cortical spheroids exposed to MP1 and MP10 at different concentrations during day 4–30, RT-PCR analysis was performed (Fig. 8 and Supplementary Table S2-S3). *ATF4* and *PAX6* were replaced by more mature neural markers *TUBB3* and *TBR1*. For *CAT* and *SOD2*, MP1 and MP10 at 5 μg/mL downregulated the expression (0.4–0.5 fold) while all the other conditions had similar expression compared to the untreated control (Fig. 8A). For *CASP3*, except that MP10 at 100 μg/mL upregulated the expression (~1.5 fold), all the other MP conditions had comparable expression compared to the control (Fig. 8B). Except for MP1 at 5 μg/mL (~0.4 fold), all the other MP conditions had comparable *CDKN1B* expression compared to the control. Similarly, MKI67 had comparable expression for all the MP conditions to the control (Fig. 8C). Except for MP10 at 100 μg/mL (~0.3 fold), all the other MP conditions had comparable *TBR2* expression compared to the control. However, for *Nestin* and *TUBB3* (encoding β-tubulin III), MP1 conditions downregulated the expression (0.5–0.7 and 0.3–0.5 respectively) (Fig. 8D). MP10 conditions showed the similar or lower *Nestin* and *TUBB3* expression. The *HOXB4* expression was comparable to the control except for MP1 at 50 μg/mL (~0.4 fold) (Fig. 8E). However, all the MP conditions downregulated *TBR1* expression (0.3–0.7 fold) compared to the control. Taken together, MP exposure may impair neural development indicated by the downregulated *TUBB3* and *TBR1* expression, although the downregulated *Nestin* expression may indicate neural maturation.

In order to identify the possible mechanism, the effects of the leachate of PS-MPs were evaluated (Supplementary Fig. S13). The

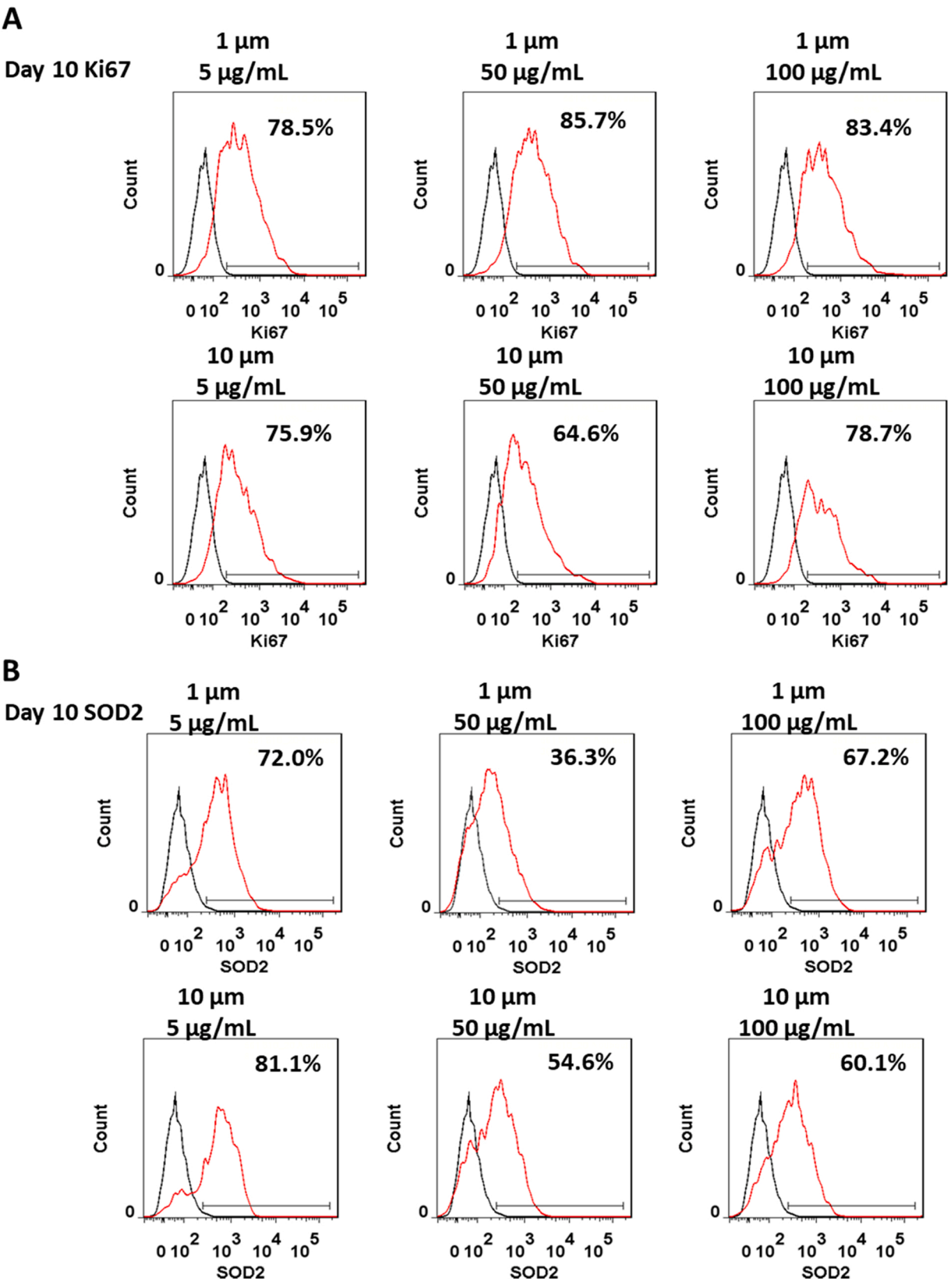

Fig. 3. Flow cytometry quantification of Ki67 and SOD2 expression in day 10 cortical spheroids exposed to microplastics (MPs). The spheroids were exposed to 1 µm and 10 µm MPs at different concentrations (5, 50, and 100 µg/mL) during day 4–10. (A) Ki67; (B) SOD2. Black line: isotype control, red line: the marker of interest.

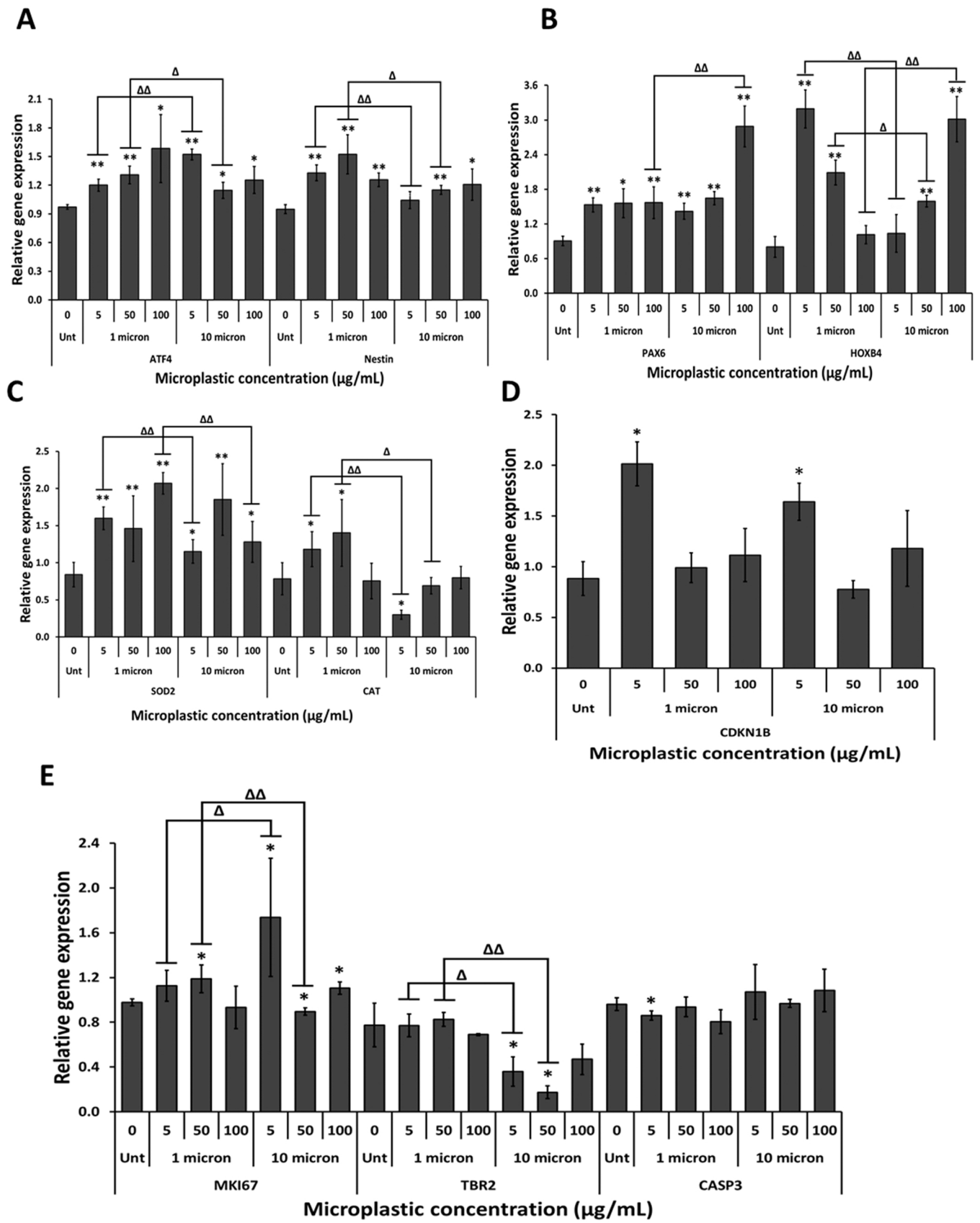

Fig. 4. The effect of MPs on the expression of various genes in day 10 cortical spheroids. RT-PCR of relative mRNA expression was performed for the following markers: (A) Neural progenitor-*ATF4* and *Nestin*; (B) Neural patterning marker-PAX6 and *HOXB4*; (C) Reactive oxygen species related-CAT and *SOD2*; (D) Cyclin-dependent kinase inhibitor 1B ($p27^{Kip1}$)-*CDKN1B*; (E) Cell proliferation-*MKI67*, Sub-ventricular region-*TBR2*, and Cellular death-*CASP3*. N = 3. * and ** indicate the statistical difference with $p < 0.05$ and $p < 0.01$, respectively, compared to the corresponding untreated control. Δ and ΔΔ indicate the statistical difference with $p < 0.05$ and $p < 0.01$, respectively, compared between the two sizes under the same concentration.

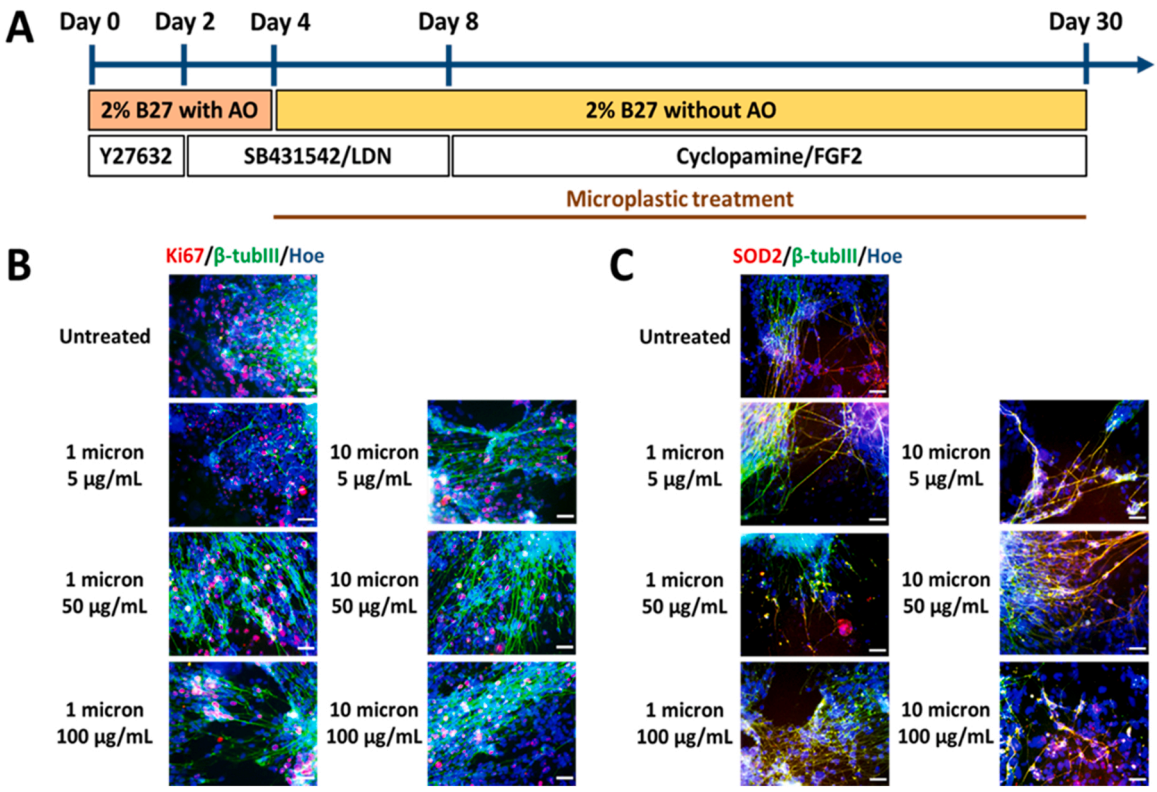

Fig. 5. Immunocytochemistry for the expression of Ki67 and SOD2 in day 30 cortical spheroids exposed to MPs. (A) The schematic illustration of forebrain cortical spheroid differentiation from hiPSCs. The spheroids were exposed to 1 μm and 10 μm MPs at different concentrations (5, 50, and 100 μg/mL) during day 4–30. Immunocytochemistry staining for (B) Ki67 and (C) SOD2 co-localized with β-tubulin III. Blue: Hoechst 33342. Scale bar: 100 μm. SOD2: superoxide dismutase 2; β-tubIII: β-tubulin isoform III.

cortical spheroids exposed to the leachate of MP1 and MP10 at 5, 50, and 100 μg/mL were examined for Ki67 (cell proliferation) and SOD2 (associated with ROS production) expression. Compared to the untreated control (78.8%), the expression of Ki67 was comparable for the conditions of MP1 at 50 μg/mL and MP10 at 5 and 50 μg/mL (80–85%). But the lower expression was observed for MP1 at 5 and 100 μg/mL (62.8% and 57.2% respectively) and MP10 at 100 μg/mL (67.4%). For SOD2, similar expression was observed for MP1 at 100 μg/mL and MP10 at 5 and 50 μg/mL (28–31%), but the lower expression was observed for MP1 at 5 and 50 μg/mL (21.9% and 18.5% respectively) and MP10 at 100 μg/mL (11.7%). These results indicate that the PS-MP leachate may contribute to the neurotoxicity of cortical spheroids.

4. Discussion

This study used hiPSC-derived forebrain cortical spheroids as a model system to study the potential threat of MP accumulation during early stages of human embryonic brain tissue development (Zarus et al., 2021). In the present study, negatively charged polystyrene MPs of 1 μm (demonstrating an intracellular mechanism) and 10 μm (demonstrating an extracellular mechanism) were evaluated for the short-term (day 4–10) and the long-term (day 4–30) exposure impacts. It is hypothesized that MPs accumulated in the cortical spheroids (either intracellularly or extracellularly) during long-time culture result in phenotypic changes in neural differentiation. During the development of cortical spheroids, MPs can get trapped between the small aggregates and later these MPs become part of the big spheroids. The 10-micron MPs stay outside the cells because of their large size, while 1-micron MPs may enter the cells via endocytosis (up to 77–81% cells may contain MP1). Our results demonstrated that the size- and concentration-dependent exposure to PS-MPs can adversely affect embryonic brain-like tissue development. To the best of our knowledge, this is the first study to assess the effects of MPs on embryonic-like tissue development of hiPSC-derived forebrain cortical spheroids.

4.1. Effects of short term (day 4–10) exposure to microplastics

Our results showed the apparent positive effects, i.e., higher expression of proliferation marker Ki67 protein and gene *MKI67*, the promoted expression of neural progenitor markers *ATF4, Nestin, PAX6,* and *HOXB4*, and the elevated *SOD2* gene expression (but not SOD2 protein), for MP exposure during day 4–10 of cortical spheroid differentiation (Fig. 9). It was postulated that MP10 and the excess MP1 provide the surface for cell adhesion in the spheroids, resulting in higher cell proliferation. The elevated *SOD2* gene expression may indicate the active ROS function. While the MP1s could be uptaken by the cells, the effects of the induced cellular stress may be compensated by the effects of the promoted cell adhesion.

The biochemical properties of the microparticles and their dimension/size should be the critical parameters to affect hPSC differentiation in 3D culture. For example, poly(lactide-co-glycolide) copolymer (PLGA) fiber microfilaments (about 250–500 μm in length and 10–20 μm in diameter) have been used as a floating scaffold to generate elongated embryoid bodies for brain organoid formation (Lancaster et al., 2017). Gelatin microparticles (1–11 μm in diameter) have been incorporated with morphogens retinoic acid and BMP2 to promote PSC aggregate differentiation (Bratt-Leal et al., 2013; Carpenedo et al., 2010). These microparticles of different biochemistry and dimension can be helpful as the scaffolds for PSC differentiation. In this study, polystyrene is non-biodegradable and cannot be eliminated from the spheroids. There are no growth factors and morphogens loaded onto PS-MPs. Therefore, the main effects during the short-term exposure may be mainly attributed to the cell-MP adhesion.

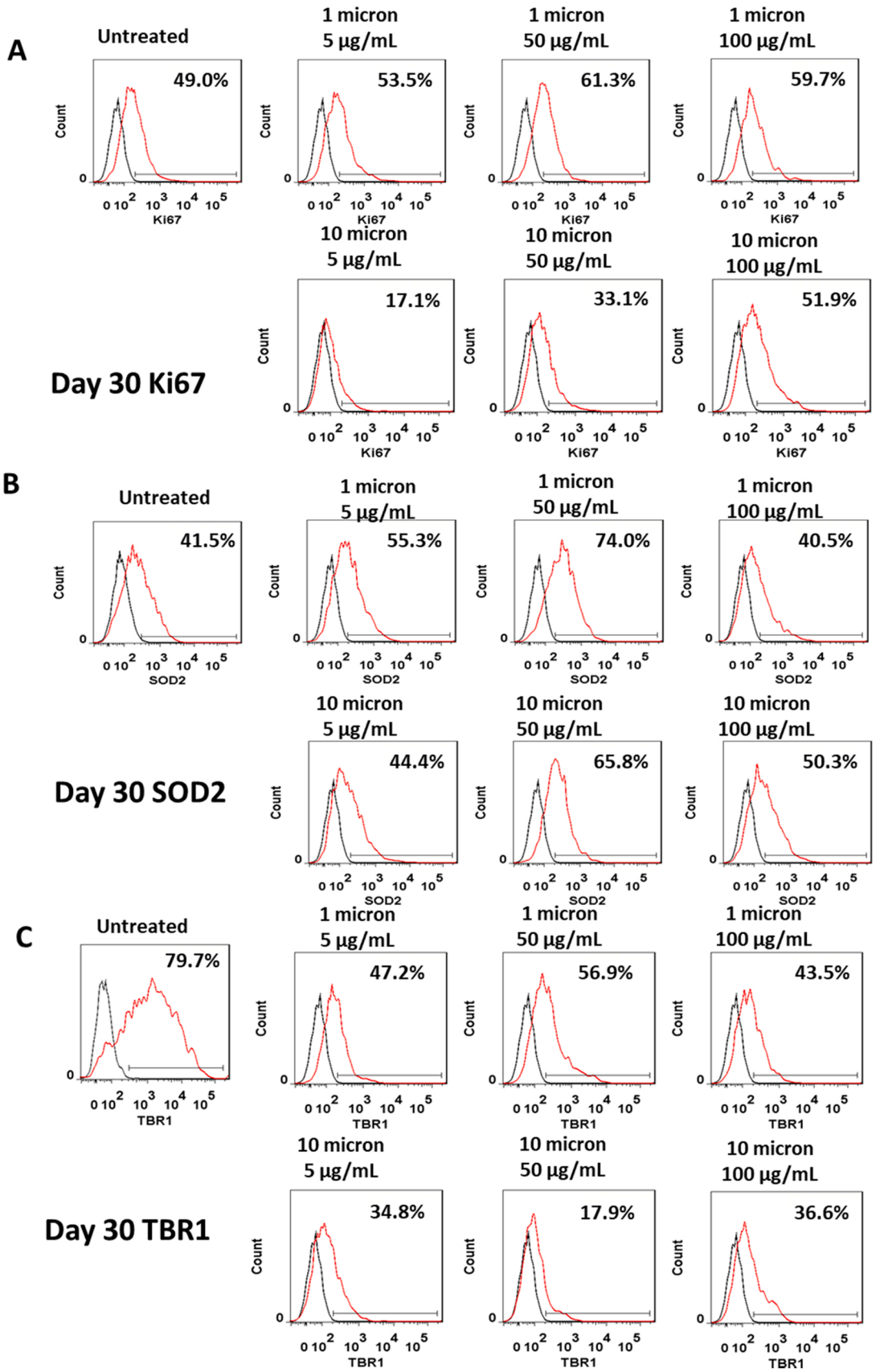

Fig. 6. Flow cytometry of Ki67, SOD2, and TBR1 expression for day 30 cortical spheroids exposed to microplastics. The spheroids were exposed to 1 μm and 10 μm MPs at different concentrations (5, 50, and 100 μg/mL) during day 4–30. (A) Ki67; (B) SOD2, and (C) TBR1. Black line: isotype control, red line: the marker of interest.

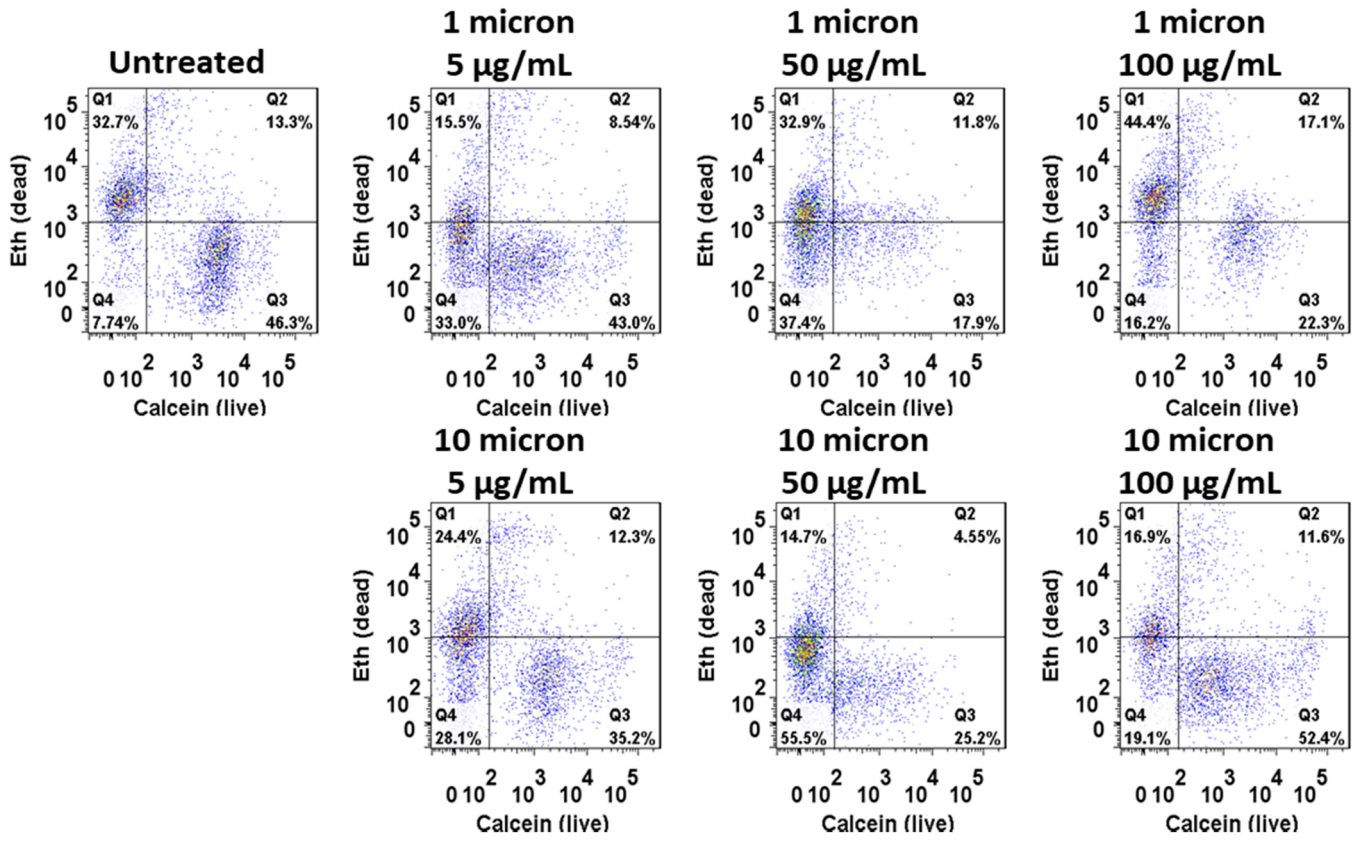

Fig. 7. Flow cytometry analysis of live and dead cells of day 30 cortical spheroids exposed to microplastics (MPs). The derived cortical spheroids were exposed to MPs during day 4–30. The cells were dissociated and stained for calcein AM and ethidium homodimer-1 as live and dead marker, respectively. These markers were analyzed using flow cytometry. Q3 (or Q2+Q3) represents the live cells, and Q1 (or Q1 +Q4) represent the dead cells. Eth: ethidium homodimer-1.

4.2. Effects of long-term (day 4–30) exposure to microplastics

Our results showed the negative effects, i.e., lower cell viability determined by Live/Dead assay, similar or lower Ki67 protein expression, down-regulation of more mature neuronal marker *TUBB3* and cortical layer VI marker *TBR1/* subventricular zone (SVZ) marker *TBR2* gene expression, for MP exposure during day 4–30 of cortical spheroid differentiation (Fig. 9). Depending on the size of MPs, different mechanisms, intracellular or extracellular, were proposed for MP1 and MP10 exposure.

Mechanism of MP1 exposure (intracellular): From our previous study, the MP1 are very likely to be uptaken (e.g., phagocytosis or endocytosis) and internalized by the neural progenitor cells (Goodman et al., 2021). Micro-sized particles of iron oxides (MPIO) can be internalized inside the neural stem cells (>70% labeling efficiency) for in vivo tracking by magnetic resonance imaging (Sart et al., 2015; Yuan et al., 2019). The dextran coating can be degraded and the released iron can go through cell metabolism to be eliminated from the cells. By contrast, the polystyrene MPs are not biodegradable and remain inside the cells after internalization. They can cause cellular stress and induce cytotoxicity, especially in long-term culture (Bhaduri et al., 2020). The MP1s did not cause significant cell death in hiPSCs but may exert toxic effects especially in long-term culture due to their efficient endocytosis (Goodman et al., 2021; Jeong et al., 2022). The intimate cell-cell interactions in cortical spheroids may not allow intracellular transport of MP1s throughout the spheroids. It was postulated that caveolae-mediated internalization may occur for MP1 uptake by the cells (Rejman et al., 2004). Accumulation of MP1s in the cells can cause gradual loss in lysosomal membrane integrity, and finally, cell death (Borkowska et al., 2020). In addition, MP1s can block essential cellular functions, including cytoskeleton formation, cellular movement, and exocytosis (Huang et al., 2010). Size-dependent (100 nm and 500 nm) effects of nanoplastics have been observed for autophagy initiation and autophagosome formation of human umbilical vein endothelial cells for 100 nm particles, whereas 500 nm particles increased lactate dehydrogenase secretion of the cells (Lu et al., 2021).

Mechanism of MP10 exposure (extracellular): From our results, MP10 exposure downregulated *TUBB3* and *TBR1/TBR2* expression. The dose-dependent response was only observed for MP10-treated day 30 cortical spheroids TBR1 and TBR2 gene expression. While MP10 cannot be uptaken by the cells, they are not biodegradable and remain inside the cortical spheroids in the extracellular spaces, affecting cell-cell adhesion and migration. It is also possible that the merging of two cortical spheroids may wrap MP10s inside the spheroids. After the initial promotion effect of cell adhesion, the non-biodegradable MP10s may interfere with the neuronal maturation and the cortical layer formation (i.e., “inside-out” embryonic brain tissue development pattern) (Bhaduri et al., 2020; Suzuki and Vanderhaeghen, 2015). The PS-MPs of 4 µm and 10 µm have also been reported to disrupt the blood-testis barrier integrity through ROS-mediated imbalance of mTORC1 and mTORC2, which may be due to the altered expression profile of actin-binding protein (Wei et al., 2021).

However, the mechanism of MP10 exposure may become complicated due to the potential breakdown of MP10s into the small particles with a size about 1 µm or nanoscale particles. While the DLS analysis showed that no MP aggregation occurs in the culture media, the long-term culture of MP10s showed the three different size of particles less than 2 µm. This process may be random and the size of broken particles may be variable (A.-U.-B. et al., 2021). Then the mechanism may shift from extracellular to the intracellular effects. In addition, the nanoscale particles may be able to pass through the blood brain barrier (BBB) and exert the detrimental effects on the brain cells. The potential effects of

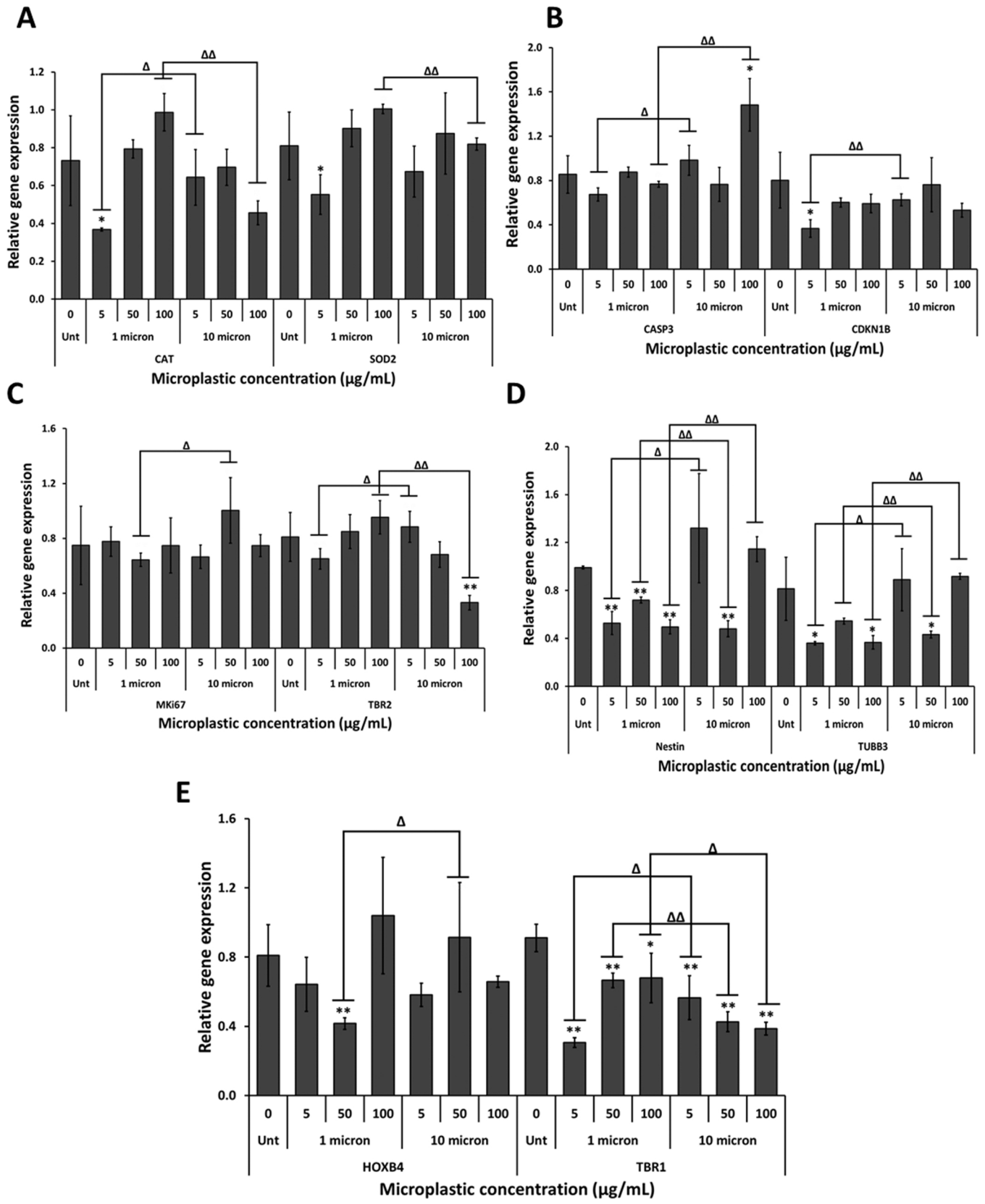

Fig. 8. The effect of MPs on the expression of various genes in day 30 cortical spheroids. RT-PCR of mRNA was performed to quantify the relative gene expression for the markers: (A) Reactive oxygen species-*CAT* and *SOD2*; (B) Cellular death-*CASP3* and Cyclin-dependent kinase inhibitor 1B (p27Kip1)-*CDKN1B*; (C) Cell proliferation-*MKI67* and Sub ventricular region marker-*TBR2*; (D) Neuronal markers-*Nestin* and *TUBB3* (β-tubulin isoform III); (E) Forebrain cortical layer VI *TBR1* and Hindbrain region-*HOXB4*. N = 3. * and ** indicate the statistical difference with $p < 0.05$ and $p < 0.01$, respectively, compared to the corresponding untreated control condition. Δ and ΔΔ indicate the statistical difference with $p < 0.05$ and $p < 0.01$, respectively, compared between the two sizes under the same concentration.

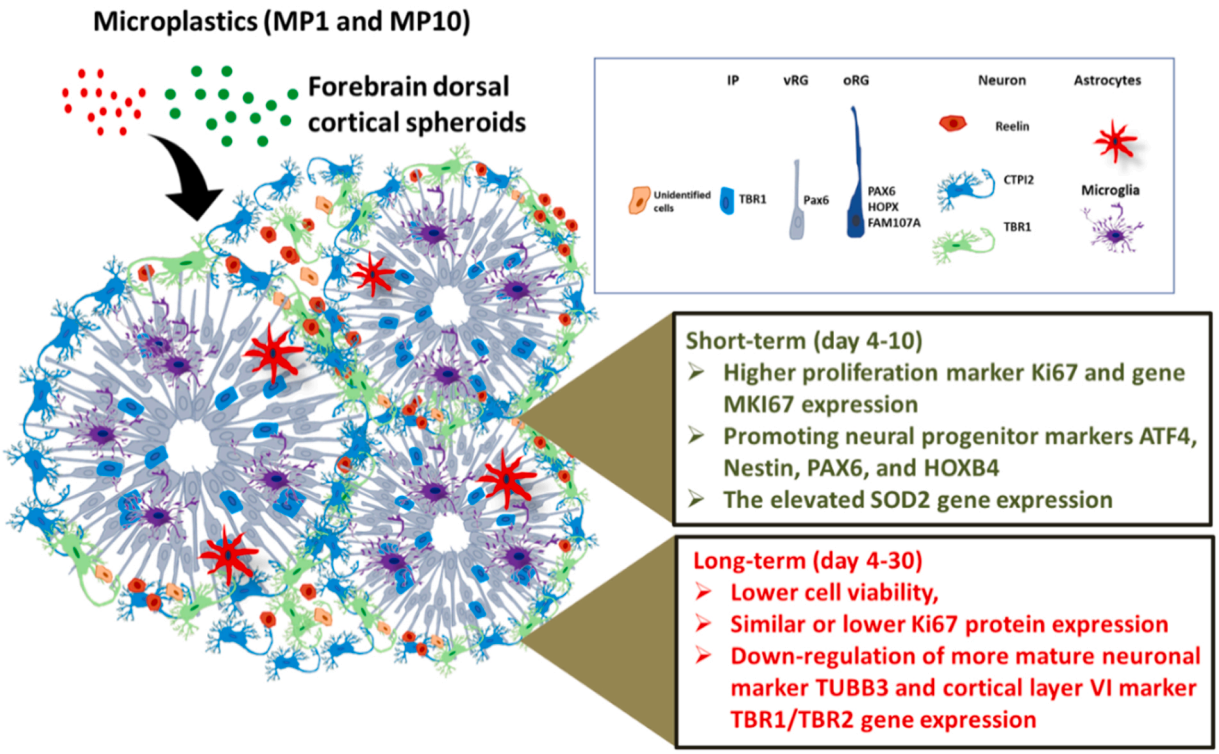

Fig. 9. Graphical results summary of MP effects on human forebrain cortical spheroids.

nanoscale plastics and their permeability in an in vitro BBB model should be further investigated in future.

Moreover, the toxicity of leachate from PS-MPs has been recognized. As the example of the identified 26 compounds in the leachate consisting of organic contaminants (PAHs) and additives, higher levels of phthalates have been detected in leachates of new plastics and the accumulation of these released hazardous chemicals over time could be one of the major contributors to the observed toxicity. (Gardon et al., 2020). In this study, the results indicate that the leachate of PS-MPs may contribute to the neurotoxicity of cortical spheroids, i.e., reduced cell proliferation and lower SOD2 expression, especially for the leachate of high amounts of PS-MPs. The leachate was prepared from the 5-day PS-MP exposure. The high concentration PS-MP group may mimic the effect of leachate accumulation over the years from the environmental level of MP exposure. The specific types of chemicals and their concentrations in the leachate need further investigations in future.

5. Conclusion

The results of quantitative and qualitative measurements in this study suggest that the size and concentration-dependent effects of PS-MPs on developing forebrain cerebral spheroids may induce high intercellular/intracellular stress and adversely affect cortical layer differentiation. While short-term MP exposure promotes cell proliferation and neural progenitor gene expression, the long-term MP exposure reduces cell viability and downregulates more mature neuronal marker and cortical layer VI marker expression. This study has significance in assessing environmental factors in neurotoxicity and degeneration and provides important insights on the health impact of environmental microplastic materials.

CRediT authorship contribution statement

Timothy Hua: Conceptualization, Methodology, Data curation, Investigation. **Sonia Kiran:** Methodology, Data curation, Writing – original draft, Investigation. **Yan Li:** Methodology, Resources, Writing – original draft, Writing – review & editing, Supervision, Project administration, Funding acquisition. **Qing-Xiang Amy Sang:** Conceptualization, Methodology, Resources, Writing – review & editing, Supervision, Project administration, Funding acquisition.

Declaration of Competing Interest

The authors declare that they have no known competing financial interests or personal relationships that could have appeared to influence the work reported in this paper.

Data Availability

The datasets generated during and/or analyzed during the current study are available from the corresponding authors on reasonable request.

Acknowledgement

The authors would like to thank Dr. Brian K. Washburn and Kristina Poduch in FSU Department of Biological Sciences for their help with RT-PCR analysis, and FSU Department of Biomedical Sciences for the support on flow cytometry analysis. This research has also used resources provided by the Materials Characterization Laboratory at the FSU Department of Chemistry and Biochemistry (FSU075000MAC), under the supervision of Dr. Raaj Vellore Winfred. The authors would also like to thank Dr. Hedi Mattoussi and Narjes Dridi at FSU Department of Chemistry and Biochemistry for their insights and help with the DLS experiments, and Dr. Joan Hare for discussions and suggestions on some aspects of the experiments. This work was mainly supported by the Council on Research & Creativity (CRC) planning grant from the Florida State University, Pfeiffer Professorship for Cancer Research in Chemistry and Biochemistry from the College of Arts & Sciences, and an Endowed Chair Professorship in Cancer Research from anonymous donors (to QXS). It is also partially supported by the Florida Department of Health (FDOH) Live Like Bella award (9LA01 to QXS and YL) and by an NSF

Career Award (No. 1652992 to YL).

Declaration of interest statement

No competing financial interests exist.

Appendix A. Supporting information

Supplementary data associated with this article can be found in the online version at doi:10.1016/j.jhazmat.2022.128884.

References

Abrahams, P.W., 2002. Soils: their implications to human health. Sci. Total Environ. 291, 1–32. https://doi.org/10.1016/S0048-9697(01)01102-0.

Ahmad, E., Feng, Y., Qi, J., Fan, W., Ma, Y., He, H., Xia, F., Dong, X., Zhao, W., Lu, Y., et al., 2017. Evidence of nose-to-brain delivery of nanoemulsions: cargoes but not vehicles. Nanoscale 9, 1174–1183. https://doi.org/10.1039/C6NR07581A.

Barboza, L.G.A., Vieira, L.R., Branco, V., Figueiredo, N., Carvalho, F., Carvalho, C., Guilhermino, L., 2018. Microplastics cause neurotoxicity, oxidative damage and energy-related changes and interact with the bioaccumulation of mercury in the European seabass, Dicentrarchus labrax (Linnaeus, 1758). Aquat. Toxicol. 195, 49–57. https://doi.org/10.1016/j.aquatox.2017.12.008.

Barboza, L.G.A., Lopes, C., Oliveira, P., Bessa, F., Otero, V., Henriques, B., Raimundo, J., Caetano, M., Vale, C., Guilhermino, L., 2020. Microplastics in wild fish from North East Atlantic Ocean and its potential for causing neurotoxic effects, lipid oxidative damage, and human health risks associated with ingestion exposure. Sci. Total Environ. 717, 134625 https://doi.org/10.1016/j.scitotenv.2019.134625.

Bejoy, J., Song, L., Wang, Z., Sang, Q.X., Zhou, Y., Li, Y., 2018a. Neuroprotective activities of heparin, heparinase iii, and hyaluronic acid on the Aβ42-treated forebrain spheroids derived from human stem cells. ACS Biomater. Sci. Eng. 4, 2922–2933. https://doi.org/10.1021/acsbiomaterials.8b00021.

Bejoy, J., Song, L., Zhou, Y., Li, Y., 2018b. Wnt/Yes-Associated protein interactions during neural tissue patterning of human induced pluripotent stem cells. Tissue Eng. Part A 24, 546–558. https://doi.org/10.1089/ten.tea.2017.0153.

Bhaduri, A., Andrews, M.G., Mancia Leon, W., Jung, D., Shin, D., Allen, D., Jung, D., Schmunk, G., Haeussler, M., Salma, J., et al., 2020. Cell stress in cortical organoids impairs molecular subtype specification. Nature 578, 142–148. https://doi.org/10.1038/s41586-020-1962-0.

Borkowska, M., Siek, M., Kolygina, D.V., Sobolev, Y.I., Lach, S., Kumar, S., Cho, Y.K., Kandere-Grzybowska, K., Grzybowski, B.A., 2020. Targeted crystallization of mixed-charge nanoparticles in lysosomes induces selective death of cancer cells. Nat. Nanotechnol. 15, 331–341. https://doi.org/10.1038/s41565-020-0643-3.

Bratt-Leal, A.M., Nguyen, A.H., Hammersmith, K.A., Singh, A., McDevitt, T.C., 2013. A microparticle approach to morphogen delivery within pluripotent stem cell aggregates. Biomaterials 34, 7227–7235 https://dx.doi.org/10.1016%2Fj.biomaterials.2013.05.079.

Carpenedo, R.L., Seaman, S.A., McDevitt, T.C., 2010. Microsphere size effects on embryoid body incorporation and embryonic stem cell differentiation. J. Biomed. Mater. Res. A 94, 466–475. https://doi.org/10.1002/jbm.a.32710.

Cederquist, G.Y., Asciolla, J.J., Tchieu, J., Walsh, R.M., Cornacchia, D., Resh, M.D., Studer, L., 2019. Specification of positional identity in forebrain organoids. Nat. Biotechnol. 37, 436–444. https://doi.org/10.1038/s41587-019-0085-3.

Chandrasekaran, K., Giordano, T., Brady, D.R., Stoll, J., Martin, L.J., Rapoport, S.I., 1994. Impairment in mitochondrial cytochrome oxidase gene expression in Alzheimer disease. Brain Res. Mol. Brain Res. 24, 336–340. https://doi.org/10.1016/0169-328x(94)90147-3.

Chen, Q., Yin, D., Jia, Y., Schiwy, S., Legradi, J., Yang, S., Hollert, H., 2017. Enhanced uptake of BPA in the presence of nanoplastics can lead to neurotoxic effects in adult zebrafish. Sci. Total Environ. 609, 1312–1321. https://doi.org/10.1016/j.scitotenv.2017.07.144.

Chiaradia, I., Lancaster, M.A., 2020. Brain organoids for the study of human neurobiology at the interface of in vitro and in vivo. Nat. Neurosci. 23, 1496–1508. https://doi.org/10.1038/s41593-020-00730-3.

Corcoran, P.L., 2020. Degradation of microplastics in the environment. Handb. Micro Environ. 1–12. https://doi.org/10.1007/978-3-030-10618-8_10-1.

Dehghani, S., Moore, F., Akhbarizadeh, R., 2017. Microplastic pollution in deposited urban dust, Tehran metropolis, Iran. Environ. Sci. Pollut. Res. 24, 20360–20371. https://doi.org/10.1007/s11356-017-9674-1.

Del Dosso, A., Urenda, J.P., Nguyen, T., Quadrato, G., 2020. Upgrading the physiological relevance of human brain organoids. Neuron 107, 1014–1028. https://doi.org/10.1016/j.neuron.2020.08.029.

Ding, J., Zhang, S., Razanajatovo, R.M., Zou, H., Zhu, W., 2018. Accumulation, tissue distribution, and biochemical effects of polystyrene microplastics in the freshwater fish red tilapia (Oreochromis niloticus). Environ. Pollut. 238, 1–9. https://doi.org/10.1016/j.envpol.2018.03.001.

Dong, C.-D., Chen, C.-W., Chen, Y.-C., Chen, H.-H., Lee, J.-S., Lin, C.-H., 2020. Polystyrene microplastic particles: In vitro pulmonary toxicity assessment. J. Hazard. Mater. 385, 121575 https://doi.org/10.1016/j.jhazmat.2019.121575.

Fetoni, A.R., Paciello, F., Rolesi, R., Pisani, A., Moleti, A., Sisto, R., Troiani, D., Paludetti, G., Grassi, C., 2021. Styrene targets sensory and neural cochlear function through the crossroad between oxidative stress and inflammation. Free Radic. Biol. Med. 163, 31–42. https://doi.org/10.1016/j.freeradbiomed.2020.12.001.

Fournier, S.B., D'Errico, J.N., Adler, D.S., Kollontzi, S., Goedken, M.J., Fabris, L., Yurkow, E.J., Stapleton, P.A., 2020. Nanopolystyrene translocation and fetal deposition after acute lung exposure during late-stage pregnancy. Part. Fibre Toxicol. 17, 1–11. https://doi.org/10.1186/s12989-020-00385-9.

Franzellitti, S., Canesi, L., Auguste, M., Wathsala, R.H., Fabbri, E., 2019. Microplastic exposure and effects in aquatic organisms: a physiological perspective. Environ. Toxicol. Pharmacol. 68, 37–51. https://doi.org/10.1016/j.etap.2019.03.009.

Freeman, L.R., Keller, J.N., 2012. Oxidative stress and cerebral endothelial cells: regulation of the blood–brain-barrier and antioxidant based interventions. Biochim. Biophys. Acta 1822, 822–829. https://doi.org/10.1016/j.bbadis.2011.12.009.

Gardon, T., Huvet, A., Paul-Pont, I., Cassone, A.L., Sham Koua, M., Soyez, C., Jezequel, R., Receveur, J., Le Moullac, G., 2020. Toxic effects of leachates from plastic pearl-farming gear on embryo-larval development in the pearl oyster Pinctada margaritifera. Water Res. 179, 115890 https://doi.org/10.1016/j.watres.2020.115890.

Garreta, E., Kamm, R.D., Chuva de Sousa Lopes, S.M., Lancaster, M.A., Weiss, R., Trepat, X., Hyun, I., Montserrat, N., 2021. Rethinking organoid technology through bioengineering. Nat. Mater. 20, 145–155. https://doi.org/10.1038/s41563-020-00804-4.

Goodman, K.E., Hare, J.T., Khamis, Z.I., Hua, T., Sang, Q.A., 2021. Exposure of human lung cells to polystyrene microplastics significantly retards cell proliferation and triggers morphological changes. Chem. Res. Toxicol. 34, 1069–1081. https://doi.org/10.1021/acs.chemrestox.0c00486.

Henderson, E., Hua, T., Kiran, S., Khamis, Z.I., Li, Y., Sang, Q.A., 2022. Long-term effects of nanoscale magnetite on human stem cell-derived cortical spheroids. ACS Biomater. Sci. Eng. 8, 801–813. https://doi.org/10.1021/acsbiomaterials.1c01487.

Huang, X., Teng, X., Chen, D., Tang, F., He, J., 2010. The effect of the shape of mesoporous silica nanoparticles on cellular uptake and cell function. Biomaterials 31, 438–448. https://doi.org/10.1016/j.biomaterials.2009.09.060.

Jeong, H., Kim, W., Choi, D., Heo, J., Han, U., Jung, S.Y., Park, H.H., Hong, S.-T., Park, J. H., Hong, J., 2022. Potential threats of nanoplastic accumulation in human induced pluripotent stem cells. Chem. Eng. J. 427, 131841 https://doi.org/10.1016/j.cej.2021.131841.

Kyrousi, C., Cappello, S., 2020. Using brain organoids to study human neurodevelopment, evolution and disease. Wiley Interdiscip. Rev. Dev. Biol. 9, e347 https://doi.org/10.1002/wdev.347.

Lancaster, M.A., Corsini, N.S., Wolfinger, S., Gustafson, E.H., Phillips, A.W., Burkard, T. R., Otani, T., Livesey, F.J., Knoblich, J.A., 2017. Guided self-organization and cortical plate formation in human brain organoids. Nat. Biotechnol. 35, 659–666. https://doi.org/10.1038/nbt.3906.

Lei, L., Liu, M., Song, Y., Lu, S., Hu, J., Cao, C., Xie, B., Shi, H., He, D., 2018. Polystyrene (nano) microplastics cause size-dependent neurotoxicity, oxidative damage and other adverse effects in Caenorhabditis elegans. Environ. Sci. Nano 5, 2009–2020. https://doi.org/10.1039/C8EN00412A.

Liang, Y., Li, J., Lin, Q., Huang, P., Zhang, L., Wu, W., Ma, Y., 2017. Research progress on signaling pathway-associated oxidative stress in endothelial cells. Oxid. Med. Cell. Longev. 2017, 7156941 https://doi.org/10.1155/2017/7156941.

Lim, J., Yeap, S.P., Che, H.X., Low, S.C., 2013. Characterization of magnetic nanoparticle by dynamic light scattering. Nanoscale Res. Lett. 8, 381 https://dx.doi.org/10.1186%2F1556-276X-8-381.

Long, M., Paul-Pont, I., Hegaret, H., Moriceau, B., Lambert, C., Huvet, A., Soudant, P., 2017. Interactions between polystyrene microplastics and marine phytoplankton lead to species-specific hetero-aggregation. Environ. Pollut. 228, 454–463. https://doi.org/10.1016/j.envpol.2017.05.047.

Lu, L., Wan, Z., Luo, T., Fu, Z., Jin, Y., 2018. Polystyrene microplastics induce gut microbiota dysbiosis and hepatic lipid metabolism disorder in mice. Sci. Total Environ. 631, 449–458. https://doi.org/10.1016/j.scitotenv.2018.03.051.

Lu, Y.Y., Li, H., Ren, H., Zhang, X., Huang, F., Zhang, D., Huang, Q., Zhang, X., 2021. Size-dependent effects of polystyrene nanoplastics on autophagy response in human umbilical vein endothelial cells. J. Hazard. Mater. 421, 126770 https://doi.org/10.1016/j.jhazmat.2021.126770.

Luo, T., Zhang, Y., Wang, C., Wang, X., Zhou, J., Shen, M., Zhao, Y., Fu, Z., Jin, Y., 2019. Maternal exposure to different sizes of polystyrene microplastics during gestation causes metabolic disorders in their offspring. Environ. Pollut. 255, 113122 https://doi.org/10.1016/j.envpol.2019.113122.

Mammo, F., Amoah, I., Gani, K., Pillay, L., Ratha, S., Bux, F., Kumari, S., 2020. Microplastics in the environment: interactions with microbes and chemical contaminants. Sci. Total Environ. 743, 140518 https://doi.org/10.1016/j.scitotenv.2020.140518.

Marzano, M., Bou-Dargham, M.J., Cone, A.S., York, S., Helsper, S., Grant, S.C., Meckes Jr., D.G., Sang, Q.X., Li, Y., 2021. Biogenesis of extracellular vesicles produced from human stem cell-derived cortical spheroids exposed to iron oxides. ACS Biomater. Sci. Eng. 7, 1111–1122. https://doi.org/10.1021/acsbiomaterials.0c01286.

Maurer, I., Zierz, S., Möller, H.J., 2000. A selective defect of cytochrome c oxidase is present in brain of Alzheimer disease patients. Neurobiol. Aging 21, 455–462. https://doi.org/10.1016/s0197-4580(00)00112-3.

Mendes, J., Curralo, A., Curado, A., Lopes, S.I., 2021. The Sustainable Smartbottle: A Proposed Design Methodology to Minimize Plastic Pollution. In: Martins, N., Brandão, D. (Eds.), Advances in Design and Digital Communication. Digicom 2020. Springer Series in Design and Innovation, 12. Springer, Cham. https://doi.org/10.1007/978-3-030-61671-7_27.

Meyer, K.C., Sharma, B., Kaufmann, B., Kupper, A., Hodgson, M., 2018. Lung disease associated with occupational styrene exposure. Am. J. Ind. Med. 61, 773–779. https://doi.org/10.1002/ajim.22867.

Miloradovic, D., Pavlovic, D., Jankovic, M.G., Nikolic, S., Papic, M., Milivojevic, N., Stojkovic, M., Ljujic, B., 2021. Human embryos, induced pluripotent stem cells, and organoids: models to assess the effects of environmental plastic pollution. Front. Cell Dev. Biol. 9, 709183 https://doi.org/10.3389/fcell.2021.709183.

Mistry, A., Glud, S.Z., Kjems, J., Randel, J., Howard, K.A., Stolnik, S., Illum, L., 2009. Effect of physicochemical properties on intranasal nanoparticle transit into murine olfactory epithelium. J. Drug Target. 17, 543–552. https://doi.org/10.1080/10611860903055470.

Nagy, Z., Esiri, M., LeGris, M., Matthews, P., 1999. Mitochondrial enzyme expression in the hippocampus in relation to Alzheimer-type pathology. Acta Neuropathol. 97, 346–354. https://doi.org/10.1007/s004010050997.

Prüst, M., Meijer, J., Westerink, R.H.S., 2020. The plastic brain: neurotoxicity of micro- and nanoplastics. Part Fibre Toxicol. 17, 1–16. https://doi.org/10.1186/s12989-020-00358-y.

Qu, M., Wang, D., 2020. Toxicity comparison between pristine and sulfonate modified nanopolystyrene particles in affecting locomotion behavior, sensory perception, and neuronal development in Caenorhabditis elegans. Sci. Total Environ. 703, 134817 https://doi.org/10.1016/j.scitotenv.2019.134817.

Rafiee, M., Dargahi, L., Eslami, A., Beirami, E., Jahangiri-rad, M., Sabour, S., Amereh, F., 2018. Neurobehavioral assessment of rats exposed to pristine polystyrene nanoplastics upon oral exposure. Chemosphere 193, 745–753. https://doi.org/10.1016/j.chemosphere.2017.11.076.

Ragusa, A., Svelato, A., Santacroce, C., Catalano, P., Notarstefano, V., Carnevali, O., Papa, F., Rongioletti, M.C.A., Baiocco, F., Draghi, S., 2021. Plasticenta: first evidence of microplastics in human placenta. Environ. Int. 146, 106274 https://doi.org/10.1016/j.envint.2020.106274.

Rejman, J., Oberle, V., Zuhorn, I.S., Hoekstra, D., 2004. Size-dependent internalization of particles via the pathways of clathrin- and caveolae-mediated endocytosis. Biochem. J. 377, 159–169. https://doi.org/10.1042/BJ20031253.

Rice, D., Barone Jr, S., 2000. Critical periods of vulnerability for the developing nervous system: evidence from humans and animal models. Environ. Health Perspect. 108, 511–533. https://doi.org/10.1289/ehp.00108s3511.

Rochman, C.M., 2018. Microplastics research—from sink to source. Science 360, 28–29. https://doi.org/10.1126/science.aar7734.

Sart, S., Calixto Bejarano, F., Baird, M.A., Yan, Y., Rosenberg, J.T., Ma, T., Grant, S.C., Li, Y., 2015. Intracellular labeling of mouse embryonic stem cell-derived neural progenitor aggregates with micron-sized particles of iron oxide. Cytotherapy 17, 98–111. https://doi.org/10.1016/j.jcyt.2014.09.008.

Sheng, L., Ze, Y., Wang, L., Yu, X., Hong, J., Zhao, X., Ze, X., Liu, D., Xu, B., Zhu, Y., 2015. Mechanisms of TiO_2 nanoparticle-induced neuronal apoptosis in rat primary cultured hippocampal neurons. J. Biomed. Mater. Res. A. 103, 1141–1149. https://doi.org/10.1002/jbm.a.35263.

Singh, A., Kukreti, R., Saso, L., Kukreti, S., 2019. Oxidative stress: a key modulator in neurodegenerative diseases. Molecules 24, 1583. https://doi.org/10.3390/molecules24081583.

Si-Tayeb, K., Noto, F.K., Sepac, A., Sedlic, F., Bosnjak, Z.J., Lough, J.W., Duncan, S.A., 2010. Generation of human induced pluripotent stem cells by simple transient transfection of plasmid DNA encoding reprogramming factors. BMC Dev. Biol. 10, 1–10. https://doi.org/10.1186/1471-213X-10-81.

Si-Tayeb, K., Noto, F.K., Nagaoka, M., Li, J., Battle, M.A., Duris, C., North, P.E., Dalton, S., Duncan, S.A., 2010. Highly efficient generation of human hepatocyte–like cells from induced pluripotent stem cells. Hepatology 51, 297–305. https://doi.org/10.1002/hep.23354.

Song, L., Wang, K., Li, Y., Yang, Y., 2016. Nanotopography promoted neuronal differentiation of human induced pluripotent stem cells. Colloids Surf. B Biointerfaces 148, 49–58. https://doi.org/10.1016/j.colsurfb.2016.08.041.

Song, L., Yuan, X., Jones, Z., Griffin, K., Zhou, Y., Ma, T., Li, Y., 2019a. Assembly of human stem cell-derived cortical spheroids and vascular spheroids to model 3-D brain-like tissues. Sci. Rep. 9, 5977. https://doi.org/10.1038/s41598-019-42439-9.

Song, L., Yuan, X., Jones, Z., Vied, C., Miao, Y., Marzano, M., Hua, T., Sang, Q.X., Guan, J., Ma, T., et al., 2019b. Functionalization of brain region-specific spheroids with isogenic microglia-like cells. Sci. Rep. 9, 11055. https://doi.org/10.1038/s41598-019-47444-6.

Stock, V., Bohmert, L., Lisicki, E., Block, R., Cara-Carmona, J., Pack, L.K., Selb, R., Lichtenstein, D., Voss, L., Henderson, C.J., et al., 2019. Uptake and effects of orally ingested polystyrene microplastic particles in vitro and in vivo. Arch. Toxicol. 93, 1817–1833. https://doi.org/10.1007/s00204-019-02478-7.

Suzuki, I.K., Vanderhaeghen, P., 2015. Is this a brain which i see before me? Modeling human neural development with pluripotent stem cells. Development 142, 3138–3150. https://doi.org/10.1242/dev.120568.

Vardhan, P.V., Shukla, L.I., 2018. FT-IR investigations on effect of high doses of gamma radiation-induced damage to polystyrene and mechanism of formation of radiolysis products. Radiat. Environ. Biophys. 57, 301–310. https://doi.org/10.1007/s00411-018-0740-y.

Velasco, S., Kedaigle, A.J., Simmons, S.K., Nash, A., Rocha, M., Quadrato, G., Paulsen, B., Nguyen, L., Adiconis, X., Regev, A., et al., 2019. Individual brain organoids reproducibly form cell diversity of the human cerebral cortex. Nature 570, 523–527. https://doi.org/10.1038/s41586-019-1289-x.

Wei, Y., Zhou, Y., Long, C., Wu, H., Hong, Y., Fu, Y., Wang, J., Wu, Y., Shen, L., Wei, G., 2021. Polystyrene microplastics disrupt the blood-testis barrier integrity through ROS-Mediated imbalance of mTORC1 and mTORC2. Environ. Pollut. 289, 117904 https://doi.org/10.1016/j.envpol.2021.117904.

Wu, C., Zhao, W., Yu, J., Li, S., Lin, L., Chen, X., 2018. Induction of ferroptosis and mitochondrial dysfunction by oxidative stress in PC12 cells. Sci. Rep. 8, 574. https://doi.org/10.1038/s41598-017-18935-1.

Xie, X., Deng, T., Duan, J., Xie, J., Yuan, J., Chen, M., 2020. Exposure to polystyrene microplastics causes reproductive toxicity through oxidative stress and activation of the p38 MAPK signaling pathway. Ecotoxicol. Environ. Saf. 190, 110133 https://doi.org/10.1016/j.ecoenv.2019.110133.

Yan, Y., Martin, L.M., Bosco, D.B., Bundy, J.L., Nowakowski, R.S., Sang, Q.-X.A., Li, Y., 2015. Differential effects of acellular embryonic matrices on pluripotent stem cell expansion and neural differentiation. Biomaterials 73, 231–242. https://doi.org/10.1016/j.biomaterials.2015.09.020.

Yan, Y., Bejoy, J., Xia, J., Guan, J., Zhou, Y., Li, Y., 2016. Neural patterning of human induced pluripotent stem cells in 3-D cultures for studying biomolecule-directed differential cellular responses. Acta Biomater. 42, 114–126. https://doi.org/10.1016/j.actbio.2016.06.027.

Yan, Y., Song, L., Bejoy, J., Zhao, J., Kanekiyo, T., Bu, G., Zhou, Y., Li, Y., 2018a. Modelling neurodegenerative microenvironment using cortical organoids derived from human stem cells. Tissue Eng. Part A 24, 1125–1137. https://doi.org/10.1089/ten.TEA.2017.0423.

Yan, Y., Song, L., Madinya, J., Ma, T., Li, Y., 2018b. Derivation of cortical spheroids from human induced pluripotent stem cells in a suspension bioreactor. Tissue Eng. Part A 24, 418–431. https://doi.org/10.1089/ten.TEA.2016.0400.

Yin, L., Chen, B., Xia, B., Shi, X., Qu, K., 2018. Polystyrene microplastics alter the behavior, energy reserve and nutritional composition of marine jacopever (Sebastes schlegelii). J. Hazard. Mater. 360, 97–105. https://doi.org/10.1016/j.jhazmat.2018.07.110.

Yuan, J., Ma, J., Sun, Y., Zhou, T., Zhao, Y., Yu, F., 2020. Microbial degradation and other environmental aspects of microplastics/plastics. Sci. Total Environ. 715, 136968 https://doi.org/10.1016/j.scitotenv.2020.136968.

Yuan, X., Rosenberg, J.T., Liu, Y., Grant, S.C., Ma, T., 2019. Aggregation of human mesenchymal stem cells enhances survival and efficacy in stroke treatment. Cytotherapy 21, 1033–1048. https://doi.org/10.1016/j.jcyt.2019.04.055.

Zarus, G.M., Muianga, C., Hunter, C.M., Pappas, R.S., 2021. A review of data for quantifying human exposures to micro and nanoplastics and potential health risks. Sci. Total Environ. 756, 144010 https://doi.org/10.1016/j.scitotenv.2020.144010.